

Platinum Electrocatalysts Deposited onto Composite Carbon Black–Metal Oxide Support

I. N. Novomlinskiy^{a, *}, V. E. Guterman^a, M. V. Danilenko^a, and V. A. Volochaev^a

^a*Southern Federal University, Rostov-on-Don, 344090 Russia*

**e-mail: novomlinskiy@sfedu.ru*

Received January 23, 2018; revised December 19, 2018; accepted February 6, 2019

Abstract—New nanostructured Pt/(SnO₂/C)-electrocatalyst (20 wt % Pt) is synthesized via platinum chemical deposited onto composite SnO₂/C-support microparticles (4 wt % Sn). The composite support was prepared beforehand using unique method of the tin electrochemical deposition onto disperse carbon black particles. It was shown by X-ray diffraction and transmission electron microscopy that the platinum and tin oxide nanoparticles distributed over the carbon surface are sized 2.4 and 2.9 nm, respectively. Electrochemical measurements showed the obtained catalyst to approach the commercial Pt/C HiSPEC 3000 catalyst (20 wt % Pt) with respect to its mass-activity in the oxygen electroreduction reaction and to be superior thereto as for the electrochemically active surface area, stability in stress test, and activity in methanol electrooxidation reaction. The peculiarities in electrochemical behavior of the synthesized Pt/(SnO₂/C)-electrocatalyst can be explained by the SnO₂ nanoparticle effect on the platinum nanoparticle nucleation/growth, as well as presence of Pt–SnO₂–C triple junction nanostructure at the surface. The Pt/SnO₂ contact provides stable platinum-to-support adhesion and asserts bifunctional catalysis mechanism of the methanol electrooxidation. And the Pt/C junctions provide for electron supplying/retraction to or from the platinum nanoparticles.

Keywords: fuel cell, Pt/SnO₂/C-electrocatalyst, Pt-nanoparticles, durability, non-carbon support, oxygen electroreduction reaction

DOI: 10.1134/S1023193519070097

INTRODUCTION

Low-temperature polymer-membrane-based fuel cells are perspective power generation plants owing to their high effectiveness in the chemical-to-electrical energy conversion, autonomy, and low air pollution [1–3]. Platinum-containing materials are the most commonly used electrocatalysts in the low-temperature fuel cells. Unfortunately, the platinum high price and limited abundance restrict the platinum-containing material usage significantly [4–7]. And this calls for the activity in the developing of new catalytically active materials for the low-temperature fuel cells, as well as the improving of existing ones.

Of particular importance is search for the catalysts combining high activity toward oxygen (electro)reduction reaction (ORR) and stability [8, 9] because kinetic difficulties in the ORR lower the low-temperature fuel cell voltage significantly, and oxygen per se and its reduction intermediate products lead to the catalyst degradation. Nowadays, some suggestions are at hand, which allow lowering the Pt content in the catalyst, increasing its activity in the ORR and stability [10]. For example, effective catalysts were prepared by Pt doping with transition *d*-metals [11, 12] and metal oxides substitution for carbonaceous support [13–17]. The oxide materials serving as more stable alternative

to carbonaceous supports can increase the catalytic activity as a result of electronic interaction with the deposited platinum nanoparticles [14, 18–23]. Tin dioxide (SnO₂) is extensively studied more recently as a perspective non-carbon support [24–27]. Unfortunately, low electron conductivity of the material restricts from its application as a support. Additionally, it is not clear how a high-porosity catalytic layer of the Pt/SnO₂-catalyst in membrane electrode assembly (MEA) can be realized. In this connection, of great interest are SnO₂-based composite systems containing porous electron-conducting phase: carbon black [28, 29], carbon nanotubes [30] etc. SnO₂ particles in composition with carbon were shown [24–26, 31, 32] to be able increasing Pt electrocatalytic activity in ORR because of electronic interaction between Pt and SnO₂, which arises due to formation of triple-junction structures: Pt–SnO₂–C. Strengthening of the platinum nanoparticles' adhesion to the support caused by their strong interaction with SnO₂-nanoparticles increases the Pt/(SnO₂/C)-catalyst stability significantly in rapid stress-tests as compared with the Pt/C-analog [32].

Most methods of the tin oxide nanoparticle deposition onto carbon support surface are based on the tin compound hydrolysis reaction [31, 33]. Electrochem-

ical methods of the SnO_2/C -materials production can be rather perspective because they allow controlling surface morphology and the obtained product purity. In particular, tin oxide was prepared by the tin metal electrochemical dispersing under the conditions of industrial-frequency alternative current application [34, 35]. Tin particles formed during the electrode sputtering precipitated on the carbon surface and were spontaneously oxidized to SnO_2 . As a result, the obtained composites contained tin dioxide nanoparticles sized 15–20 nm. Subsequent platinum deposition onto the composition support particles allowed obtaining $\text{Pt}/(\text{SnO}_2 + \text{C})$ -catalyst whose highest activity in the CO oxidation reaction was observed at a minor (2–5 wt %) SnO_2 content. Part of the platinum nanoparticles anchored at larger tin dioxide nanoparticles is likely to be electrically isolated; on this reason, increase of tin dioxide fraction in the material over 5% has a negative effect on the catalyst activity in the methanol and CO electrooxidation reactions. The platinum activity increase in the presence of SnO_2 was explained [34, 35] by the electrocatalysis bifunctional mechanism: hydroxyl groups adsorbed at SnO_2 surface facilitate oxidation of the CO molecules adsorbed at the platinum nanoparticles surface.

In view of the above, inference should be drawn that the two-component SnO_2/C -supports are very perspective in the producing of deposited platinum electrocatalysts under the conditions of the platinum nanoparticles anchoring at the tin dioxide/carbon interface. By contrast, the platinum anchoring at the SnO_2 surface in the absence of electrical contact with carbon can lead to their deactivation in the electrocatalysis.

The present work is based on the following hypothesis: the using of the composite SnO_2/C -support containing tin dioxide as small-sized nanoparticles for the subsequent platinum nanoparticles deposition allows obtaining three-phase $\text{Pt}/(\text{SnO}_2/\text{C})$ -electrocatalysts in which, on the one hand, electron supplying/removal to or from the platinum nanoparticles is provided; on the other hand, a great part of the platinum nanoparticles contacts the tin dioxide nanoparticles directly. This work aims at the obtaining of such a material by original method of electrodeposition, studying of its based platinum-containing catalyst electrochemical behavior in ORR and the methanol electrooxidation reaction, as compared with the commercial Pt/C -catalyst.

EXPERIMENTAL

Synthesis of SnO_2/C

The SnO_2/C -materials were prepared by original procedure. The two-electrode electrochemical cell was filled with a disperse carbon material suspension based on tin(II) chloride solution. The suspension was

obtained by the mixing of Vulcan XC72 carbon black (Cabot Corporation, USA; the specific surface area $270 \text{ m}^2 \text{ g}^{-1}$) with 1 M tin(II) chloride solution (reagent grade) prepared on the basis of 1 M H_2SO_4 . The mixture was dispersed in a Sonics ultrasonic homogenizer for 2 min; then, it was continuously stirred with a magnetic stirrer to keep it homogeneous. Electrodes were immersed into the suspension. The cathode was copper wire with the working surface area of 0.5 cm^2 ; the anode, a graphite rod. The electrolysis was carried out under the suspension intense stirring, by passing dc of 9 A.

The carbon microparticles, touching the cathode in the process of stirring, actually became its part. Tin ions were electroreduced at the microparticles, forming nanosized tin crystals. During the electrolysis, great number of the carbon support repeatedly touched the stationary cathode; on this reason, the tin particles nucleation/growth processes occurs at their surface. constant renewal of the carbon nanoparticles in the electron-conducting near-cathode layer caused by the forced convection resulted in a more-or-less uniform distribution of the electrodeposited tin over the carbon support microparticles' surface (see the "Results and Discussion" section). Apparently, the tin nanoparticles were partly oxidized by dissolved oxygen right in the process of preparation, thus converting to tin(IV) oxide particles.

Upon completion of the electrolysis the suspension was filtered, the precipitate was repeatedly washed by twice distilled water up to the achieving of the neutral reaction of the medium and dried in a drying oven at 80°C within 24 h. Tin nanoparticles deposited onto the carbon support and remained unoxidized now became oxidized in the process of filtering and drying thus forming tin dioxide nanoparticles.

The Vulcan XC72 carbon support suspension was subjected to similar treatment in 1 M H_2SO_4 solution by passing dc of 9 A. Pt/C -catalyst obtained after the platinum deposition onto this carbon support was used as a reference.

Preparation of $\text{Pt}/(\text{SnO}_2/\text{C})$ and Pt/C

The $\text{Pt}/(\text{SnO}_2/\text{C})$ - and Pt/C -catalysts were synthesized by H_2PtCl_6 chemical reduction from liquid phase as described in [36], in suspension containing carbon or the composite SnO_2/C -support particles. The calculated Pt mass fraction in $\text{Pt}/(\text{SnO}_2/\text{C})$ is 20%. To this purpose, the powdered support obtained upon completing the electrolysis was put to 20 mL of ethylene glycol, then added the required amount of $\text{H}_2[\text{PtCl}_6] \cdot 6\text{H}_2\text{O}$. Thus obtained suspension was homogenized using ultrasound, then consecutively added 0.5 mL of 37% HCOH and 1 M NaOH solution in a water–ethylene glycol mixture (1 : 1) up to the achieving of pH 11. After a 2-h exposure to a temperature of 90°C and spontaneous cooling of the stirred

suspension it was added with 20 mL of 1 M NaCl, a sedimentation agent.

In 30 min the mixture was filtered through a Buchner funnel, washed 5–6 times by twice distilled water and ethanol, and then dried at 80°C.

Research Methods

To determine the composition of the SnO₂/C-, Pt/C-, and Pt/(SnO₂/C)-materials and detect tin dioxide and platinum crystallites therein we used X-ray diffraction and thermogravimetric analysis. Powder X-ray diffraction patterns of the metal- and carbon-oxide-materials were registered with an ARL X'TRA automatic diffractometer (Thermo Fisher Scientific, Switzerland) (Bragg–Brentano geometry, radius 260 mm, vertical theta–theta goniometer) using a copper K_α-radiation ($\lambda = 1.5418 \text{ \AA}$). Typical operation characteristics: 40 kV, 30 mA, sampling interval 0.02 degree. The sample rate was varied from 2 deg/min (in the routine X-ray diffraction analyses) to 0.5 deg/min (in the refining of the structure details). Standard polycrystalline α -quartz plate served as a calibration standard.

The obtained diffraction patterns were used in the tin dioxide and platinum detection in the materials, as well as determining of the crystallite average size (diameter) of both platinum [by using the (111) reflexion] and tin dioxide [by using the (101) peak]. The D value was calculated by the Scherrer formula to which the full width at half maximum for the corresponding peak was substituted: $D = K\lambda/(FWHM\cos\theta)$, where λ is the monochromatic radiation wavelength (\AA), $FWHM$ is the full width at half maximum (radians), D is the crystallite average size (nm), θ is the reflection angle, $K = 0.89$ is the Scherrer constant.

The tin dioxide $\omega(\text{SnO}_2)$ and platinum mass fractions in SnO₂/C and Pt/(SnO₂/C) were determined by using thermogravimetric method from the residual mass of SnO₂ or (Pt + SnO₂) after burning down of carbon (800°C, 40 min).

The platinum-to-tin ratio in the studied materials was determined by X-ray fluorescence analysis using an ARL OPTIM'X spectrometer (Thermo Fisher Scientific, Switzerland).

To measure the electrochemical active platinum surface area we used cyclic voltammetry. Thin layer of platinum-containing material was applied to end face of rotating disc electrode. To this purpose, 6 μL of the Pt/(SnO₂/C)- or Pt/C-containing suspension and Nafion polymer additive applied to end face of glassy carbon disc electrode. After drying, to fasten the powder porous layer, another 7 μL of 0.05% Nafion solution in isopropanol was deposited, and then the electrode was dried for 15 min at room temperature. An AFCBP1 potentiostat (Pine Applied Instrumentation, USA) was used in the imposing of the potential scanning and the current recording.

Initially, to standardize the Pt surface and fully remove impurities, 100 cycles of the potential scanning was applied in the potential interval from 0 to 1 V at a rate of 200 mV s⁻¹. Then, two cyclic voltammograms were registered over the potential interval from 0.03 to 1.20 V at a potential scan rate of 20 mV s⁻¹. Further, from the charge consumed in the atomic hydrogen electrochemical adsorption and desorption in the 2nd cyclic voltammogram we calculated the electrochemical active surface area, as described earlier [37]. An Ag/AgCl/KCl-electrode served as a reference electrode. Below, all potential values will be given against reversible hydrogen electrode (RHE).

In the calculating of the electrochemical active platinum surface area from the charge consumed in the chemisorbed CO monolayer oxidation, we passed CO through the solution at the potential of 0.45 V for 20 min; then argon, for 30 min. Subsequently, two cyclic voltammograms were recorded in the potential interval from 0.03 to 1.20 V at a potential scan rate of 20 mV s⁻¹.

To evaluate the catalyst activity in ORR, a series of voltammograms were recorded with linear potential scanning in the potential interval from 0.02 to 1.2 V at a potential scan rate of 20 mV s⁻¹ and the disc electrode rotation velocity of 400, 900, 1600, and 2500 rpm. The potential (E) values were corrected for the Ohmic voltage loss in the cell by the following formula: $E = E_{\text{reg}} - iR$, where E_{reg} is the registered potential value (V), i is the current at this potential (A), R is the electrolyte resistance (Ω). The measured electrolyte resistance is 25 Ω , which corresponds well to the literature data [38]. Additionally, we subtracted the background curve measured in the Ar-saturated electrolyte, as it was described earlier [39]. The kinetic current and the number of electrons participating in the reaction were calculated by the Koutecký–Levich equation [40]:

$$1/i = 1/i_k + 1/i_d = 1/i_k + 1/Z\omega^{0.5},$$

$$Z = 0.62nFD^{2/3}\nu^{-1/6}c,$$

where i is the current to the disc electrode (A cm⁻²); i_k is the kinetic current (A cm⁻²); i_d is the diffusion current (A cm⁻²); ω is the disc electrode rotation velocity (rad s⁻¹); n is the number of electrons participating in the oxygen molecule electroreduction reaction; F is the Faraday constant (C mol⁻¹); D is the diffusion coefficient (cm² s⁻¹); ν is the electrolyte kinematic viscosity (cm² s⁻¹); and c is the oxygen concentration in the solution (mol cm⁻³).

To evaluate the catalyst stability, we used the voltammetric cycling method, which was applied in the three-electrode cell over the potential range from 0.6 to 1.4 V at a potential scan rate of 100 mV/s. The cycling was carried out in 0.1 M HClO₄ solution in Ar atmosphere at 25°C for 2000 cycles; after each 100 cycles, two cyclic voltammograms were recorded

at a potential scan rate of 20 mV/s over the potential range from -0.03 to 1.20 V. The 2nd cyclic voltammogram was used in the calculating of the surface area (S) according to the procedure described earlier. The stability was evaluated by changes in the S_j/S_0 ratio, where j is the number of the stress-test cycles, as well as by the S_{2000}/S_0 value.

The catalyst activity in the methanol oxidation reaction was evaluated by using cyclic voltammetry and potentiostatic chronoamperometry methods ($E = 0.8$ V) in the electrolyte containing 0.5 M CH_3OH in 0.1 M HClO_4 as supporting solution.

Transmission electron microscopy (TEM)-microphotographs were obtained using a JEM-2100 microscope (JEOL, Japan) working at a voltage of 200 kV; the resolving power was 0.2 nm. To perform the measurements, 0.5 mg of Pt/C was put into 1 mL of isopropanol and dispersed by ultrasound. A drop of the suspension was applied to copper mesh coated with amorphous carbon layer, and dried in air at room temperature for 20 min.

RESULTS AND DISCUSSION

The tin electrodeposition onto carbon black microparticles gave SnO_2/C -materials with the tin mass fraction from 4 to 40 wt %. The X-ray diffraction analysis of the materials confirmed the presence of therein (Fig. 1). The increase of the SnO_2 mass fraction in the material results in the increase of intensity of the peaks characteristic of the tin(IV) oxide (Fig. 1). The X-ray diffraction pattern of the sample containing 40 wt % of SnO_2 also shows narrow peaks that point to the presence of the tin crystalline phase that in all probability has been fallen down from the cathode surface.

The tin oxide scanning-electron-microscopy-examination was carried out with the SnO_2/C sample containing 40 wt % of tin oxide.

Analysis of the images (Fig. 2) showed that the tin electrocrystallization and the nanocrystal subsequent oxidation resulted in the formation of tin dioxide nanoparticles on the carbonaceous support surface, which are well uniformly distributed over the carbon microparticles' surface. Their average size is approximately 2.9 nm. Thus, the method of tin electrocrystallization on carbon particles in their suspension, developed by us for the SnO_2/C -material preparation allows obtaining tin dioxide nanoparticles of lesser size than the earlier described synthetic methods [31, 32, 34, 35].

When examining cyclic voltammograms of the SnO_2/C -materials, we did not detect any Faradaic processes involving oxidation of the tin metal residue or Sn(IV) reduction. The main difference in the cyclic voltammograms, observed when passing from a carbon electrode (Fig. 3a) to the oxide-carbon one (Fig. 3b) is the increase of absolute value of the current at the oxide-carbon material. Apparently, in the pres-

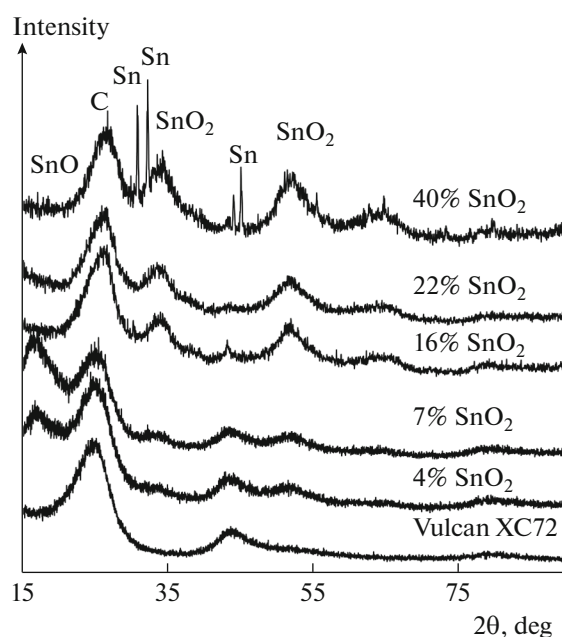


Fig. 1. X-ray diffraction patterns of the Vulcan XC72 carbon black support and SnO_2/C -materials with different tin oxide mass fraction (4 – 40 wt %).

ence of the SnO_2 nanoparticles at the carbon microparticles surface leads to increase of the material full surface area; as a result, larger charge is consumed in the processes of the electrical double layer charging–discharging.

Flat maximums in the potential range from 0.5 to 0.8 V (Fig. 3b) are characteristic of interconversion in the quinone/hydroquinone system [41, 42]. They are due to the carbonaceous support surface oxidation during the tin electrolytic deposition. In the course of the composite electrolytic production, tin is deposited onto cathode-contacting carbon black particles, thus forming the nanoparticles. The tin nanoparticles, which are thermodynamically unstable in the solution, are oxidized to tin dioxide. When the Sn/C and SnO_2/C particles touch the anode we have either the tin anodic dissolution (when and if the metal nanoparticles not yet have converted to oxide nanoparticles) or the carbon surface fragments oxidation (quinone group formation).

Because the electronic conductivity of SnO_2 is very low and the SnO_2 nanoparticles are predominantly localized at the carbon black surface, rather than in its microparticle pores, in the preparation of the deposited platinum catalyst we used composite support sample containing 4 wt % of tin oxide. When choosing the composition, we also took the results of works [34, 35] into account; they were briefly described in the “Introduction” section. The X-ray diffraction analysis of the prepared Pt/(SnO_2/C)-material confirmed the presence of platinum phase therein

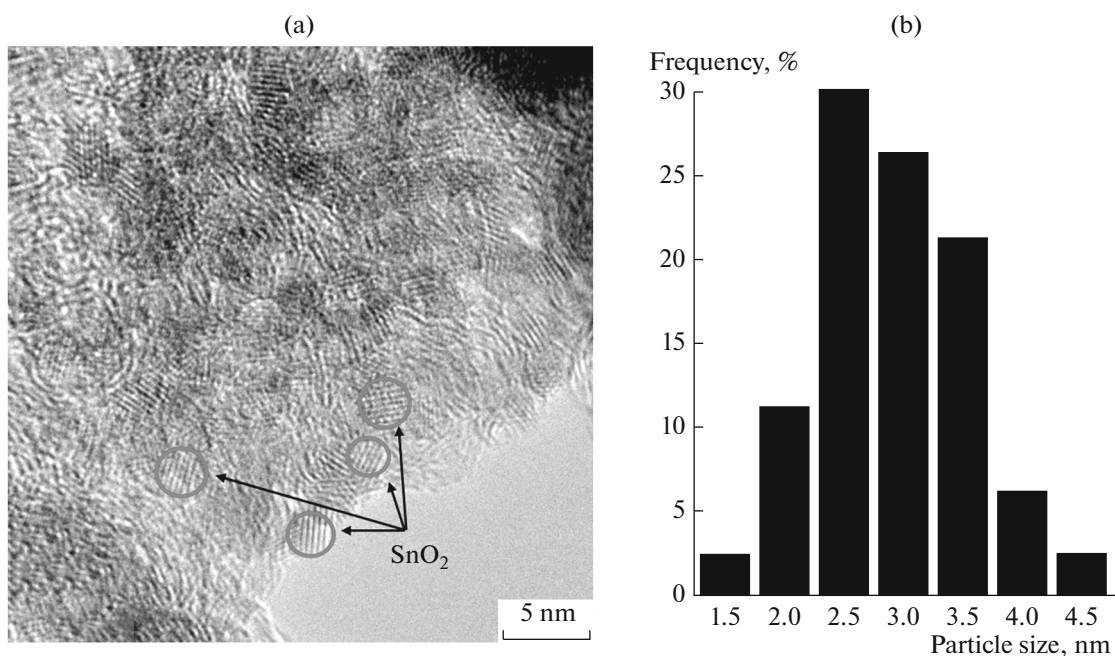


Fig. 2. Transmission electron microscopy. TEM-microphotograph of SnO₂/C-material surface fragment (a) and histogram of the SnO₂ nanoparticles distribution in size (b). SnO₂ mass fraction 40%.

(Fig. 4), with the crystallites sized 2.4 nm on the average. We note that tin dioxide wide reflexions are practically imperceptible in the X-ray diffraction patterns at a platinum background because of the tin dioxide low content in the catalyst.

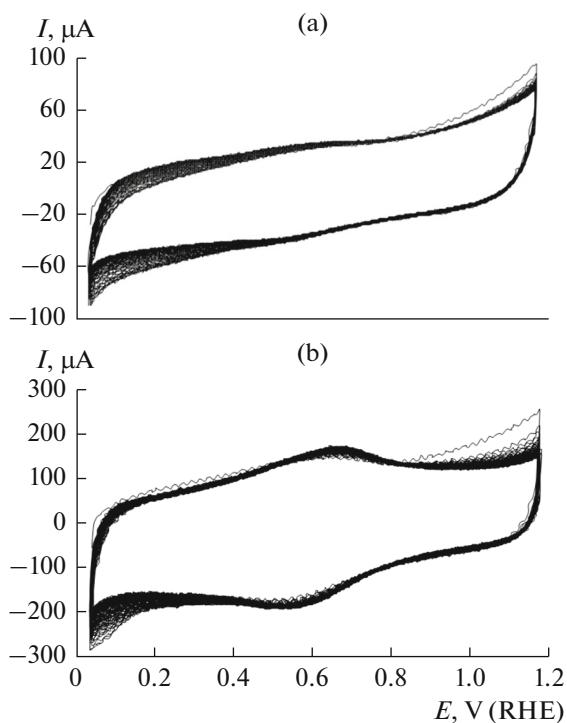


Fig. 3. Cyclic voltammograms during Vulcan XC72 (a) and SnO₂/C (b) pre-treatment.

Nonetheless, the comparison of the surface fragments microphotographs for the SnO₂/C- (Fig. 2) and Pt/(SnO₂/C)-materials (Fig. 5a) allows detecting both platinum and tin dioxide nanoparticles. The SnO₂ presence at the catalyst surface is also confirmed by the results of the energy dispersive X-ray spectroscopy (Fig. 5c). The copper reflexions in the spectrum are due to the usage of the copper mesh in the procedure of the catalyst examination (see the “Research Meth-

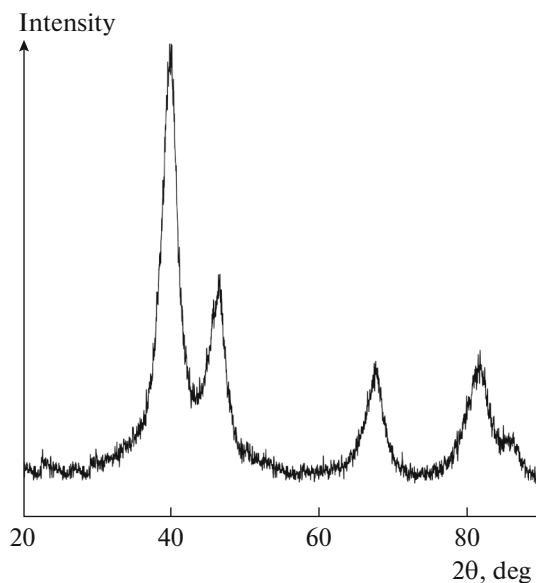


Fig. 4. X-ray diffraction pattern of Pt/(SnO₂/C) sample containing 20 wt % Pt.

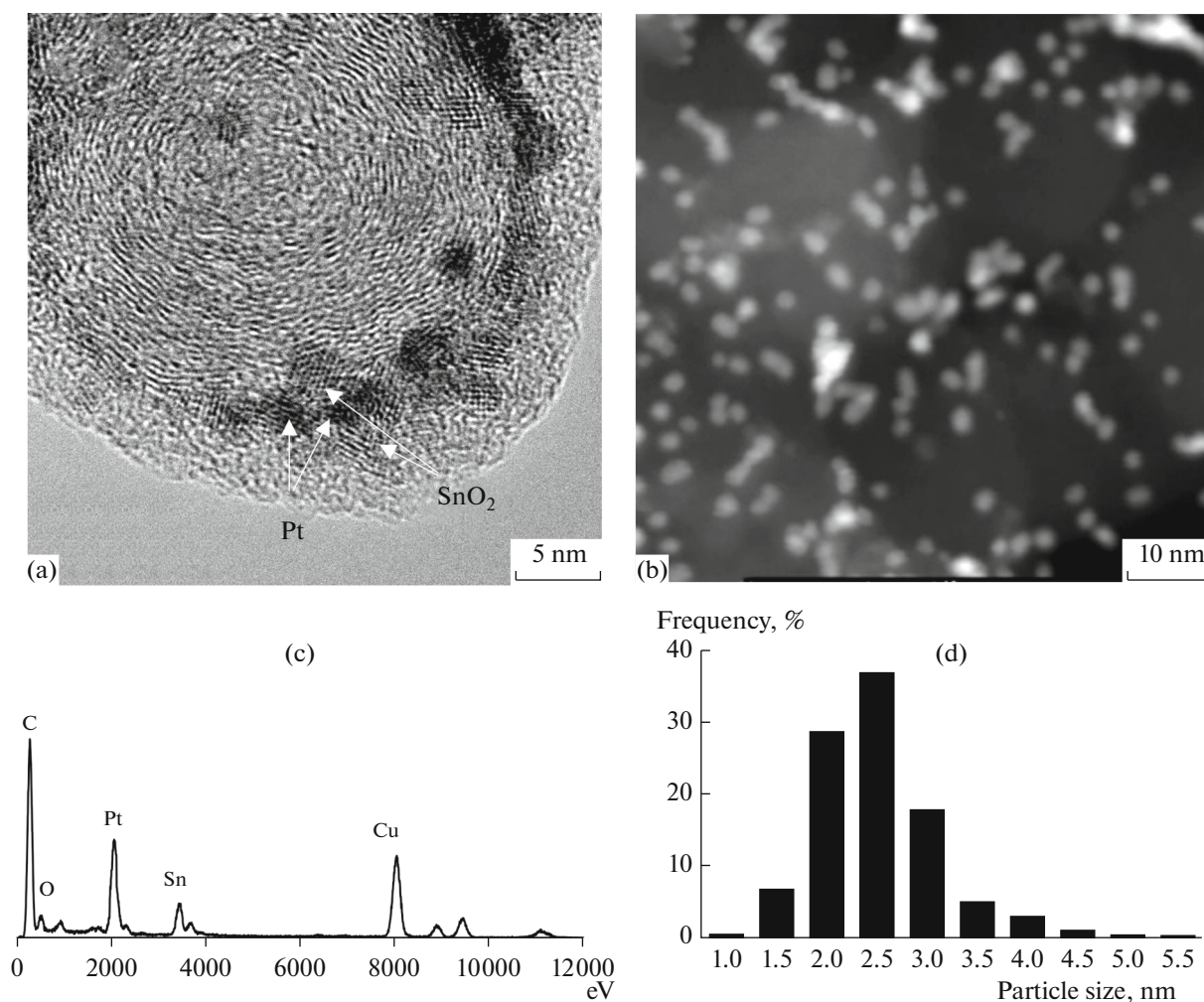


Fig. 5. TEM-microphotograph of Pt/(SnO₂/C) surface fragment (a); STEM-microphotograph of Pt/(SnO₂/C) surface (b); results of energy dispersive transmission electron microscopy analysis (c) and histogram of the platinum nanoparticles distribution in Pt/(SnO₂/C)-material (d) in Pt/(SnO₂/C)-material.

ods" section). The data obtained in STEM-mode (Fig. 5b) evidence uniform platinum nanoparticles' distribution over the catalyst surface. The nanoparticles' average size is 2.3 nm (Fig. 5d). Considerable part of the platinum nanoparticles contact both carbon and the tin oxide nanoparticles, that is, it is involved in the triple-junction zone formation.

X-ray diffraction analysis of the carbon-support-based Pt/C-catalyst treated under similar conditions revealed platinum characteristic reflexions. The platinum crystallite average size calculated from the 111 reflexion half-width by using the Scherrer equation is 1.6 nm.

The electrochemically active surface area was calculated from cyclic voltammograms recorded at the pre-treated Pt/(SnO₂/C)-electrode (see the "Experimental" section). It came to $\sim 118 \pm 12 \text{ m}^2 \text{ g}^{-1}$, which exceeds the value for the commercial Pt/C-catalyst

HiSPEC 3000 and the Pt/C-catalyst we prepared under similar conditions ($\sim 93 \pm 9$ and $101 \pm 10 \text{ m}^2 \text{ g}^{-1}$, respectively). The high value of the Pt/(SnO₂/C)-catalyst electrochemically active surface area is due, to our view, to the combination of the nanoparticles' small size and their weak agglomeration (or, what is the same, uniform spatial distribution). Also, it is not unthinkable that the presence in the triple-junction zone of certain number of small-sized (less than 1 nm) less crystalline platinum nanoparticles not detectable by the X-ray diffraction analysis and TEM methods. The electrochemically active surface area calculations by the charge consumed in the adsorbed CO oxidation confirmed that calculated by the charge consumed in the hydrogen adsorption and desorption (Fig. 6a). And this allows ruling out the version on the SnO₂ direct participation in any electrochemical reactions

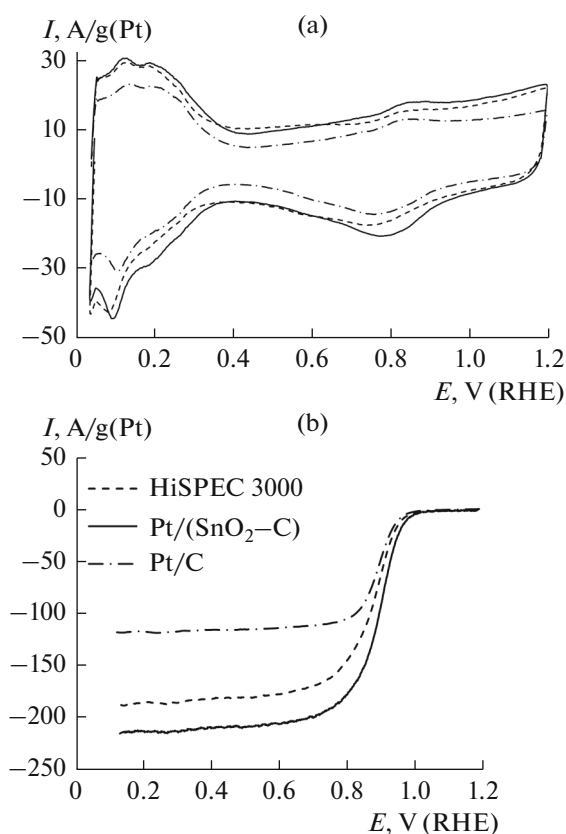


Fig. 6. Cyclic voltammograms of catalysts in Ar atmosphere (a) and voltammograms of oxygen electroreduction reaction (b).

that occur over the potential interval from 0 to 0.4 V (RHE).

The Pt/(SnO₂/C) activity in the ORR approaches that of the commercial analog (Fig. 6b): at the same half-wave potential equal to 0.90 V the kinetic current values for Pt/(SnO₂/C) and HiSPEC 3000 were 153 and 187 A/g(Pt), respectively. At that, the kinetic current value calculated for the “home made” Pt/C appeared being noticeably lower than that for the Pt/(SnO₂/C)-catalyst: 95 A/g(Pt). Taking into consideration literature data [43], one may suppose that the larger electrochemically active surface area of the Pt/(SnO₂/C)-material, as compared with that of the commercial Pt/C, does not lead to its larger mass-activity in ORR, because of larger fraction of the small-sized (2 nm and less) nanoparticles whose surface has lower specific activity [44]. At that, the composite-support-based catalyst shows a noticeably higher specific kinetic current (1.30 A/m²) as compared with that of the Pt/C on the basis of pre-treated carbon (1.02 A/m²), which evidences, even if indirectly, a tin dioxide positive effect on the platinum nanoparticles’ activity.

In stress-tests carried out over the potential range from 0.6 to 1.4 V (which corresponds to the so-called

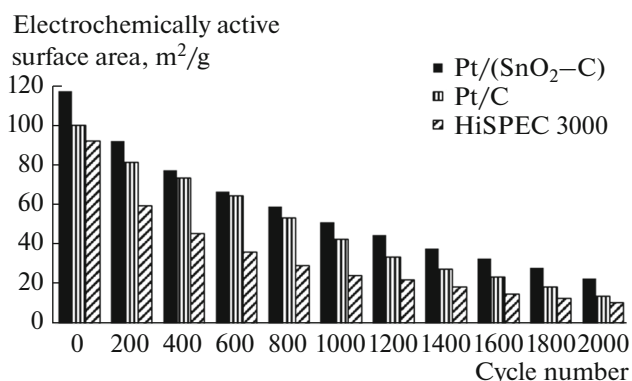


Fig. 7. Measurement of electrochemically active platinum surface area in the course of voltammetric stress-testing. Potential interval 0.6–1.4 V, potential scan rate 20 mV/s. Electrolyte: 0.1 M HClO₄ solution, Ar-saturated at atmospheric pressure.

support protocol) the Pt/(SnO₂/C)-catalyst demonstrated higher values of specific stability than the Pt/C-analogs (Fig. 7). The degradation degree of Pt/(SnO₂/C), Pt/C, and HiSPEC3000 after 2000 cycles came to 80, 86, and 88%, respectively. It is known that the platinum–carbon electrocatalysts degradation during their testing in the 0.6–1.4 V potential range is mainly due to the carbon support oxidation in the spots of its contacting platinum nanoparticles, which catalyzed the oxidation process [11, 44]. The positive effect from even small amount (~4%) of tin dioxide on the catalyst stability against the degradation can be induced both by the platinum strong adhesion to the support surface in spots of three-phase contact Pt/(SnO₂/C) and the carbon degradation deceleration in these spots. This result correlates well with the data of work [32] on a SnO₂ positive effect on the deposited platinum electrocatalyst stability under milder conditions of stress-testing.

In the light of literature data on a tin dioxide positive effect on the methanol electrooxidation reaction rate on platinum [35], we expected higher activity of SnO₂-containing catalysts when studying the reaction. Indeed, the methanol electrooxidation reaction maximal current in the direct and reverse voltammograms, as well as areas under the corresponding maximums appeared being noticeably larger for the Pt/(SnO₂/C)-catalyst than for Pt/C-analogs (Fig. 8c). When the methanol electrooxidation reaction was carried out in chronoamperometric mode at $E = 0.8$ V, the oxide-containing catalyst also demonstrated larger reaction rate throughout the measurements (Fig. 8a), which may be connected to the higher platinum surface area in the oxide-containing sample. The comparison of specific characteristics (Fig. 8b) shows that the Pt/(SnO₂/C)-catalyst activity in the methanol electrooxidation reaction at 0.80 V decreased slower than the commercial sample activity. This may evidence

Table 1. Comparison of the catalyst's electrochemically active surface area and half-wave potentials in ν ORR prior to and after stress-tests

Catalyst	Electrochemically active surface area, $\text{m}^2/\text{g}(\text{Pt})$		$E_{1/2}$, V	
	prior to	after	prior to	after
Pt/($\text{SnO}_2 + \text{C}$)	118	23	0.90	0.75
HiSPEC 3000	93	11	0.90	0.67
Pt/C	101	14	0.90	0.79

both the specificity of the platinum oxidation in Pt/(SnO_2/C) and its higher stability against poisoning with the methanol oxidation products [45]. The cur-

rent decrease on the pretreated-carbon-based Pt/C-catalyst occurs much faster. At comparable initial current values, the chronoamperogram final current for Pt/C is less than that for Pt/(SnO_2/C) by a factor of ~ 4 .

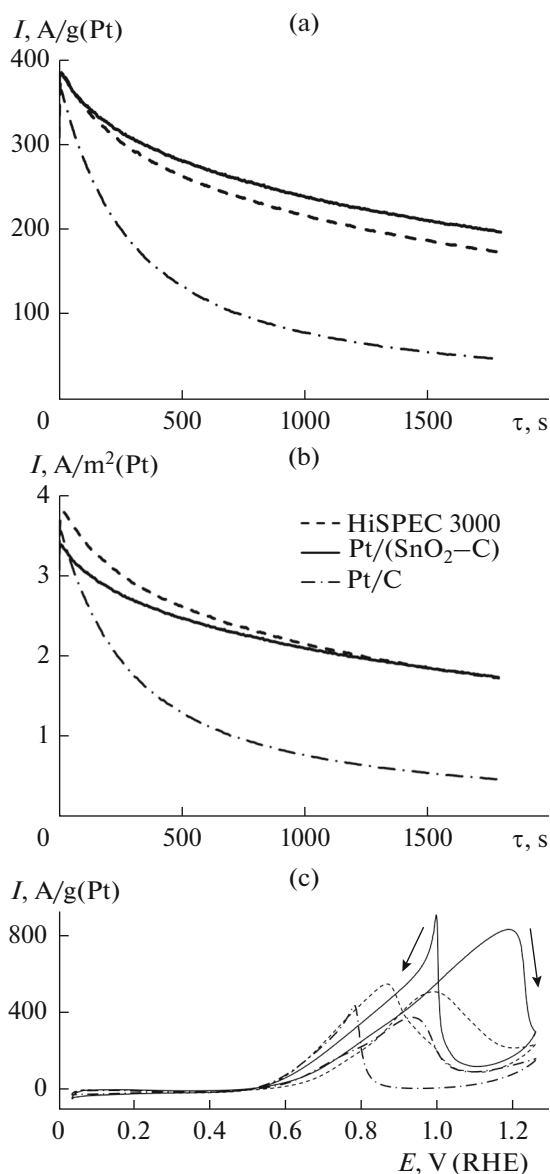


Fig. 8. Chronoamperogram recorded at $E = 0.8$ V (a, b) and cyclic voltammogram (c) of methanol oxidation reaction carried out at the studied electrocatalysts.

CONCLUSIONS

Tin nanoparticles capable of being spontaneously oxidized to SnO_2 by solution components and air oxygen were formed at the surface of disperse carbon support particles by using the method of electrodeposition. As a result, the composite SnO_2/C -materials containing 4 to 40% of tin dioxide as uniformly distributed small-sized nanoparticles with the average diameter of ~ 2.9 nm are obtained. Deposited Pt/(SnO_2/C)-electrocatalyst was prepared by chemical reduction of Pt(IV) in SnO_2/C -suspension based on the material containing 4 wt % SnO_2 .

Because the platinum and SnO_2 nanoparticles are close in size, the electrical insulation of sorbed platinum nanoparticles from carbon ones is hampered, which favors formation of Pt– SnO_2 –C triple-junction zones in the obtained Pt/(SnO_2/C)-catalyst containing about 20 wt % Pt. At the platinum nanoparticles' average size of 2.3 nm its electrochemically active surface area comes to $\sim 118 \pm 12 \text{ m}^2/\text{g}(\text{Pt})$. Thus synthesized Pt/(SnO_2/C)-catalyst demonstrated larger mass-activity in ORR and higher corrosion-morphological stability under the conditions of voltammetric cycling over the potential range from 0.6 to 1.4 V as compared with the Pt/C-material prepared under similar conditions. It is also well superior to Pt/C-analogs in its mass-activity in the methanol electrooxidation reaction. The special features of the Pt/(SnO_2/C)-catalyst electrochemical behavior can be due to the presence on its surface of great deal of platinum nanoparticles simultaneously contacting both with tin dioxide and carbon. Stronger adhesion of such nanoparticles to the composite support surface can hamper platinum degradation in the stress-testing, and the Pt/ SnO_2 contact gives rise to bifunctional catalysis mechanism in the methanol electrooxidation reaction. One more important factor affecting the Pt/(SnO_2/C)-catalyst electrochemical behavior special features can be tin dioxide nanoparticle effect on

the platinum nanoparticles nucleation/growth processes during the catalyst synthesis and, as a consequence, their more uniform spatial distribution, as well as the presence of poorly identified very small sized nanoparticles (less than 1 nm). These factors as often as not can provide high platinum electrochemically active surface area, which we have determined from atomic hydrogen and CO electrochemical desorption.

Note that the tin dioxide nanoparticles' effect on the platinum catalyst characteristics manifests itself even at its small content in the composite. Taking into account possible favorable effect of the Pt/SnO₂ contact on the catalyst functional characteristics and the negative role of the low electron conductivity of tin dioxide per se, we believe that systematic studies of the SnO₂ content on the Pt/(SnO₂/C)-catalyst electrochemical behavior can be fruitful path in optimization of their composition.

FUNDING

This study is performed within the framework of the state target of the Ministry of education and sciences of RF (topic no. 13.3005.2017/4.6).

CONFLICT OF INTEREST

The authors declare that they have no conflict of interest.

REFERENCES

1. Debe, M.K., Electrocatalyst approaches and challenges for automotive fuel cells, *Nature*, 2012, vol. 486, no. 7401, p. 43.
<https://doi.org/10.1038/nature11115>
2. Yaroslavtsev, A.B., Dobrovolsky, Yu.A., Shaglaeva, N.S., Frolova, L.A., Gerasimova, E.V., and Sanginov, E.A., Nanostructured materials for low-temperature fuel cells, *Russ. Chem. Rev.*, 2012, vol. 81, p. 191.
3. Liao, H., Qiu, Z., Wan, Q., Wang, Z., Liu, Y., and Yang, N., Universal Electrode Interface for Electrocatalytic Oxidation of Liquid Fuels, *ACS Appl. Mater. Interfaces*, 2014, vol. 6, no. 20, p. 18055.
<https://doi.org/10.1021/am504926r>
4. Gong, K., Du, F., Xia, Z., Durstock, M., and Dai, L., Nitrogen-Doped Carbon Nanotube Arrays with High Electrocatalytic Activity for Oxygen Reduction, *Science*, 2009, vol. 323, no. 5915, p. 760.
<https://doi.org/10.1126/science.1168049>
5. Jin, S., Chen, M., Dong, H., He, B., Lu, H., Su, L., Dai, W., Zhang, Q., and Zhang, X., Stable silver nanoclusters electrochemically deposited on nitrogen-doped graphene as efficient electrocatalyst for oxygen reduction reaction, *J. Power Sources*, 2015, vol. 274, p. 1173.
<https://doi.org/10.1016/j.jpowsour.2014.10.098>
6. Liu, S., Zhang, Q., Li, Y., Han, M., Gu, L., Nan, C., Bao, J., and Dai, Z., Five-Fold Twinned Pd₂NiAg Nanocrystals with Increased Surface Ni Site Availability to Improve Oxygen Reduction Activity, *J. Am. Chem. Soc.*, 2015, vol. 137, no. 8, p. 2820.
<https://doi.org/10.1021/ja5129154>
7. Ma, T.Y., Ran, J., Dai, S., Jaroniec, M., and Qiao, S.Z., Phosphorus-Doped Graphitic Carbon Nitrides Grown in situ on Carbon-Fiber Paper: Flexible and Reversible Oxygen Electrodes, *Angew. Chem. Int. Ed.* 2014, vol. 54, no. 15, p. 4646.
<https://doi.org/10.1002/anie.201411125>
8. Guterman, V.E., Belenov, S.V., Alekseenko, A.A., Tabachkova, N.Yu., and Volochaev, V.A., The relationship between activity and stability of deposited platinum-carbon electrocatalysts, *Russ. J. Electrochem.*, 2017, vol. 53, p. 531.
9. Lim, C.S., Wang, L., Chua, C.K., Sofer, Z., Jankovský, O., and Pumera, M., High temperature superconducting materials as bi-functional catalysts for hydrogen evolution and oxygen reduction, *J. Mater. Chem. A*, 2015, vol. 3, no. 16, p. 8346.
<https://doi.org/10.1039/c4ta06767c>
10. Qiao, Y. and Li, C.M., Nanostructured catalysts in fuel cells, *J. Mater. Chem.*, 2011, vol. 21, no. 12, p. 4027.
<https://doi.org/10.1039/c0jm02871a>
11. Hasche, F., Oezaslan, M., and Strasser, P., Activity, stability, and degradation mechanisms of dealloyed PtCu₃ and PtCo₃ nanoparticle fuel cell catalysts, *Chem-CatChem*, 2011, vol. 3, p. 1805.
12. Alekseenko, A.A., Belenov, S.V., Volochaev, V.A., Novomlinskiy, I.N., and Guterman, V.E., Cu@Pt/C catalysts: synthesis, structure, activity in oxygen reduction reaction, In *Advanced Materials – Techniques, Physics, Mechanics, and Applications*, Parinov, I.A., Ed. Heidelberg: Springer Proceedings in Physics, vol. 193, 2017.
13. Gojković, S., Babić, B., Radmilović, V., and Krstajić, N., 2010, Nb-doped TiO₂ as a support of Pt and Pt–Ru anode catalyst for PEMFCs, *J. Electroanal. Chem.*, vol. 639, no. 1–2, p. 161.
<https://doi.org/10.1016/j.jelechem.2009.12.004>
14. Ho, V.T.T., Pan, C.-J., Rick, J., Su, W.-N., and Hwang, B.-J., Nanostructured Ti_{0.7}Mo_{0.3}O₂ Support Enhances Electron Transfer to Pt: High-Performance Catalyst for Oxygen Reduction Reaction, *J. Am. Chem. Soc.*, 2011, vol. 133, no. 30, p. 11716.
<https://doi.org/10.1021/ja2039562>
15. Ignaszak, A., Song, C., Zhu, W., Wang, Y.-J., Zhang, J., Bauer, A., Baker, R., Neburchilov, V., Campbell, S., and Ye, S., Carbon–Nb_{0.07}Ti_{0.93}O₂ composite supported Pt–Pd electrocatalysts for PEM fuel cell oxygen reduction reaction, *Electrochim. Acta*, 2012, vol. 75, p. 220.
<https://doi.org/10.1016/j.electacta.2012.04.111>
16. Jukk, K., Kongi, N., Tarre, A., Rosental, A., Treshchalov, A., Kozlova, J., Ritslaid, P., Matisen, L., Sammelselg, V., and Tammeveski, K., Electrochemical oxygen reduction behaviour of platinum nanoparticles supported on multi-walled carbon nanotube/titanium dioxide composites, *J. Electroanal. Chem.*, 2014, vol. 735, p. 68.
<https://doi.org/10.1016/j.jelechem.2014.10.008>
17. Tiido, K., Alexeyeva, N., Couillard, M., Bock, C., Macdougall, B.R., and Tammeveski, K., Graphene–TiO₂ composite supported Pt electrocatalyst for oxygen

- reduction reaction, *Electrochim. Acta*, 2013, vol. 107, p. 509.
<https://doi.org/10.1016/j.electacta.2013.05.155>
18. Cui, X., Shi, J., Chen, H., Zhang, L., Guo, L., Gao, J., and Li, J., Platinum/Mesoporous WO_3 as a Carbon-Free Electrocatalyst with Enhanced Electrochemical Activity for Methanol Oxidation, *J. Phys. Chem. B*, 2008, vol. 112, no. 38, p. 12024.
<https://doi.org/10.1021/jp803565k>
 19. Ioroi, T., Siroma, Z., Fujiwara, N., Yamazaki, S.-I., and Yasuda, K., Sub-stoichiometric titanium oxide-supported platinum electrocatalyst for polymer electrolyte fuel cells, *Electrochem. Commun.*, 2005, vol. 7, no. 2, p. 183.
<https://doi.org/10.1016/j.elecom.2004.12.007>
 20. Lei, B., Xue, J., Jin, D., Ni, S., and Sun, H., Fabrication, annealing, and electrocatalytic properties of platinum nanoparticles supported on self-organized TiO_2 nanotubes, *Rare Metals*, 2008, vol. 27, no. 5, p. 445.
[https://doi.org/10.1016/s1001-0521\(08\)60160-6](https://doi.org/10.1016/s1001-0521(08)60160-6)
 21. Shim, J., Lee, C.-R., Lee, H.-K., Lee, J.-S., and Cairns, E.J., Electrochemical characteristics of Pt- WO_3/C and Pt- TiO_2/C electrocatalysts in a polymer electrolyte fuel cell, *J. Power Sources*, 2001, vol. 102, no. 1–2, p. 172.
[https://doi.org/10.1016/s0378-7753\(01\)00817-5](https://doi.org/10.1016/s0378-7753(01)00817-5)
 22. Vayssilov, G.N., Lykhach, Y., Migani, A., Staudt, T., Petrova, G.P., Tsud, N., Skála, T., Bruix, A., Illas, F., Prince, K.C., Matolin, V., Neyman, K.M., and Libuda, J., Support nanostructure boosts oxygen transfer to catalytically active platinum nanoparticles, *Nature Materials*, 2011, vol. 10, no. 4, p. 310.
<https://doi.org/10.1038/nmat2976>
 23. Wang, M., Guo, D.-J., and Li, H.-L., High activity of novel Pd/ TiO_2 nanotube catalysts for methanol electro-oxidation, *J. Solid State Chem.*, 2005, vol. 178, no. 6, p. 1996.
<https://doi.org/10.1016/j.jssc.2005.04.006>
 24. Dou, M., Hou, M., Liang, D., Lu, W., Shao, Z., and Yi, B., SnO_2 nanocluster supported Pt catalyst with high stability for proton exchange membrane fuel cells, *Electrochim. Acta*, 2013, vol. 92, p. 468.
<https://doi.org/10.1016/j.electacta.2013.01.070>
 25. Nakada, M., Ishihara, A., Mitsushima, S., Kamiya, N., and Ota, K.-I., Effect of Tin Oxides on Oxide Formation and Reduction of Platinum Particles, *Electrochem. Solid State Lett.*, 2007, vol. 10, no. 1.
<https://doi.org/10.1149/1.2382263>
 26. Tripković, D., Stevanović, S., Gavrilović, A., Rogan, J., Lačnjevac, U., Kravić, T., and Jovanović, V.M., The Role of SnO_2 on Electrocatalytic Activity of PtSn Catalysts, *Electrocatalysis*, 2017, vol. 9, no. 1, p. 76.
<https://doi.org/10.1007/s12678-017-0424-4>
 27. Frolova, L.A., Dobrovolsky, Y.A., and Bukun, N.G., Oxide supported platinum electrocatalysts for hydrogen and alcohol fuel cells, *Russ. J. Electrochem.*, 2011, vol. 47, no. 6, p. 697.
<https://doi.org/10.1134/s1023193511060024>
 28. Antoniassi, R., Silva, J., Neto, A.O., and Spinacé, E., Synthesis of Pt SnO_2/C electrocatalysts containing Pt nanoparticles with preferential (100) orientation for direct ethanol fuel cell, *Appl. Catal. B Environ.*, 2017, vol. 218, p. 91.
<https://doi.org/10.1016/j.apcatb.2017.06.031>
 29. Jia, J., Wang, H., Ji, S., Yang, H., Li, X., and Wang, R., SnO_2 -embedded worm-like carbon nanofibers supported Pt nanoparticles for oxygen reduction reaction, *Electrochim. Acta*, 2014, vol. 141, p. 13.
<https://doi.org/10.1016/j.electacta.2014.07.020>
 30. Huang, M., Zhang, J., Wu, C., and Guan, L., Pt nanoparticles Densely Coated on SnO_2 -Covered Multiwalled Carbon Nanotubes with Excellent Electrocatalytic Activity and Stability for Methanol Oxidation, *ACS Appl. Mater. Interfaces*, 2017, vol. 9, no. 32, p. 26921.
<https://doi.org/10.1021/acsami.7b07866>
 31. Zhang, K., Feng, C., He, B., Dong, H., Dai, W., Lu, H., and Zhang, X., An advanced electrocatalyst of Pt decorated SnO_2/C nanofibers for oxygen reduction reaction, *J. Electroanal. Chem.*, 2016, vol. 781, p. 198.
<https://doi.org/10.1016/j.jelechem.2016.11.002>
 32. Zhang, N., Zhang, S., Du, C., Wang, Z., Shao, Y., Kong, F., Lin, Y., and Yin, G., Pt/Tin Oxide/Carbon Nanocomposites as Promising Oxygen Reduction Electrocatalyst with Improved Stability and Activity, *Electrochim. Acta*, 2014, vol. 117, p. 413.
<https://doi.org/10.1016/j.electacta.2013.11.139>
 33. Parrondo, J., Mijangos, F., and Rambabu, B., Platinum/tin oxide/carbon cathode catalyst for high temperature PEM fuel cell, *J. Power Sources*, 2010, vol. 195, no. 13, p. 3977.
<https://doi.org/10.1016/j.jpowsour.2010.01.027>
 34. Kuriganova, A.B., Leontyeva, D.V., Ivanov, S., Bund, A., and Smirnova, N.V., Electrochemical dispersion technique for preparation of hybrid MO_x-C supports and Pt/ MO_x-C electrocatalysts for low-temperature fuel cells, *J. Appl. Electrochem.*, 2016, vol. 46, no. 12, p. 1245.
<https://doi.org/10.1007/s10800-016-1006-5>
 35. Kuriganova, A.B. and Smirnova, N.V., Pt/ SnO_x-C composite material for electrocatalysis, *Mendeleev Commun.*, 2014, vol. 24, no. 6, p. 351.
<https://doi.org/10.1016/j.mencom.2014.11.013>
 36. Alekseenko, A.A., Guterman, V.E., Volochaev, V.A., and Belenov, S.V., Effect of wet synthesis conditions on the microstructure and active surface area of Pt/C catalysts, *Inorg. Mater.*, 2015, vol. 51, no. 12, p. 1258.
<https://doi.org/10.1134/s0020168515120018>
 37. Guterman, V.E., Lastovina, T.A., Belenov, S.V., Tabachkova, N.Y., Vlasenko, V.G., Khodos, I.I., and Balakshina, E.N., PtM/C (M = Ni, Cu, or Ag) electrocatalysts: effects of alloying components on morphology and electrochemically active surface areas, *J. Solid State Electrochem.*, 2013, vol. 18, no. 5, p. 1307.
<https://doi.org/10.1007/s10008-013-2314-x>
 38. Vliet, D.V.D., Strmcnik, D.S., Wang, C., Stamenkovic, V.R., Markovic, N.M., and Koper, M.T., On the importance of correcting for the uncompensated Ohmic resistance in model experiments of the Oxygen Reduction Reaction, *J. Electroanal. Chem.*, 2010, vol. 647, no. 1, p. 29.
<https://doi.org/10.1016/j.jelechem.2010.05.016>
 39. Shinozaki, K., Zack, J.W., Pylypenko, S., Pivovar, B.S., and Kocha, S.S., Oxygen Reduction Reaction Measurements on Platinum Electrocatalysts Utilizing

- Rotating Disk Electrode Technique, *J. Electrochem. Soc.*, 2015, vol. 162, no. 12.
<https://doi.org/10.1149/2.0551512jes>
40. Jeon, M.K., Zhang, Y., and McGinn, P.J., A comparative study of PtCo, PtCr, and PtCoCr catalysts for oxygen electro-reduction reaction, *Electrochim. Acta*, 2010, vol. 55, no. 19, p. 5318.
<https://doi.org/10.1016/j.electacta.2010.04.056>
41. Fabbri, E., Rabis, A., Kötz, R., and Schmidt, T.J., Pt nanoparticles supported on Sb-doped SnO₂ porous structures: developments and issues, *Phys. Chem. Chem. Phys.*, 2014, vol. 16, no. 27, p. 13672.
<https://doi.org/10.1039/c4cp00238e>
42. Wang, J., Yin, G., Shao, Y., Zhang, S., Wang, Z., and Gao, Y., Effect of carbon black support corrosion on the durability of Pt/C catalyst, *J. Power Sources*, 2007, vol. 171, no. 2, p. 331.
<https://doi.org/10.1016/j.jpowsour.2007.06.084>
43. Thompsett, D., Catalysts for the proton exchange membrane fuel cell, in: *Handbook of Fuel Cells. Fundamentals, Technology and Applications*, Vielstich, W., Lamm, A., and Gasteiger, H.A., Eds., New York: Wiley, 2003, p. 6–23.
44. Park, Yu-Ch., Kakinuma, K., Uchida, M., Uchida, H., and Watanabe, M., Deleterious effects of interim cyclic voltammetry on Pt/carbon black catalyst degradation during start-up/shutdown cycling evaluation, *Electrochim. Acta*, 2014, vol. 123, p. 84.
45. Eris, S., Daşdelen, Z., and Sen, F., Enhanced electro-catalytic activity and stability of monodisperse Pt nanocomposites for direct methanol fuel cells, *J. Colloid Interface Sci.*, 2018, vol. 513, p. 767.
<https://doi.org/10.1016/j.jcis.2017.11.085>

Translated by Yu. Pleskov